Select Topics in Mass Transfer and Magnetic Braking

Kenny Van

Supervisor: Natalia Ivanova

University of Alberta

August 29, 2017

Binarity

- Initially introduced by Herschel (1802).
- Large fractions of stars have a companion (Abt and Levy, 1976; Mason et al., 1998).
- Many massive stars expected to interact (Sana et al., 2012).
- Interacting binaries source of "exotic" systems.

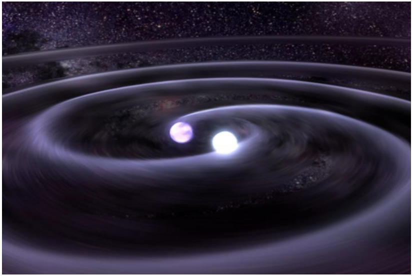

Figure: Example of a white dwarf binary.

Mass Transfer

- If the two stars in the binary are close enough together, the stars will undergo mass transfer.
- In systems where the accretor is a compact object, X-ray radiation will be emitted as mass is accreted.
- Mass transfer may be wind fed or through a process called Roche lobe overflow.

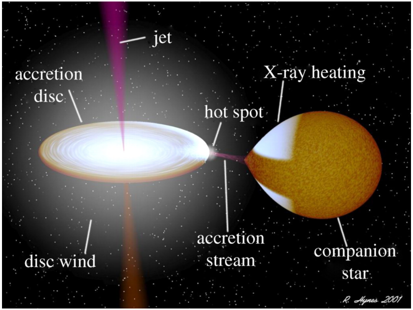

Figure: Schematic of a mass transferring binary.

Roche Lobe Description

- The Roche lobe is the region where the material of the star is gravitationally bound to it. In 1D the radius of the Roche lobe is approximated by (Eggleton, 1983):

$$\frac{\mathrm{R_{RL}}}{a} \approx \frac{0.49\mathrm{q}^{2/3}}{0.6\mathrm{q}^{2/3} + \ln(1 + \mathrm{q}^{1/3})}$$

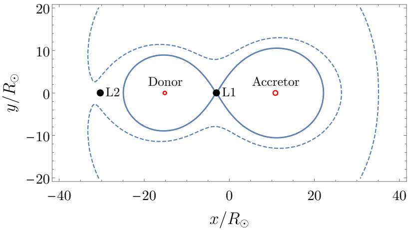

Figure: Roche lobe schematic in the x-y plane with a 1.4 $\mathrm{M}_\odot$ accretor and a 1.0 $\mathrm{M}_\odot$ donor, initial separation of 26 $\mathrm{R}_\odot$.

Roche Lobe Description

- Based on this description, we can classify the system as one of the following (Kopal, 1955):
  1. Detached System
  2. Semi-detached System
  3. Contact System
- If the system overfills the L_2 point the two stars may undergo a common envelope event.

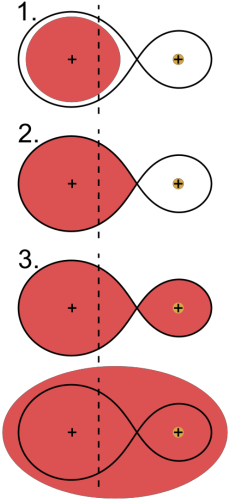

Mass Transfer Stability

- The stability of mass transfer depends on how the accretor, the donor and its Roche lobe change over the course of the evolution. The response is characterized by mass-radius exponents:

$$\xi_{\rm eq} = \left(\frac{d\ln \mathrm{R}}{d\ln \mathrm{M}}\right)_{\rm eq}, \quad \xi_{\rm RL} = \left(\frac{d\ln \mathrm{R}}{d\ln \mathrm{M}}\right)_{\rm RL}, \quad \xi_{\rm ad} = \left(\frac{d\ln \mathrm{R}}{d\ln \mathrm{M}}\right)_{\rm ad}$$

- These quantify the relative change in the radius given a change in mass.

Mass Transfer Stability

- Based on the mass-radius exponents, various inequalities denote the type mass transfer and the stability.
  1. Stable ($\xi_{\rm RL} \leq \xi_{\rm eq}$): The mass transfer is stable as the star stays within the Roche lobe as the star shrinks more quickly than the Roche lobe.
  2. Thermal ($\xi_{\rm ad} > \xi_{\rm RL} > \xi_{\rm eq}$): The mass transfer dynamically stable and self-regulating.
  3. Dynamically unstable ($\xi_{\rm RL} > \xi_{\rm ad}$): The star cannot adjust quickly enough to remain within the Roche lobe.

Adiabatic Response

- The response of the donor when $\xi_{\rm RL} > \xi_{\rm ad}$ is tied to the entropy profile of the star.
    1. A flat entropy profile corresponding with convection, results in stellar expansion and runaway mass transfer.
    2. An entropy profile decreasing with mass corresponds to a radiative layer which results in stable mass transfer.

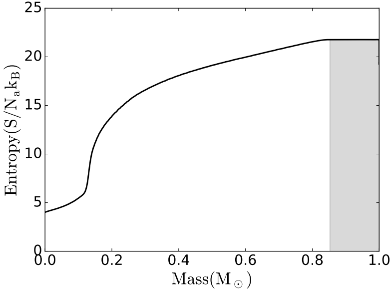

Figure: The entropy profile of a $1\ \mathrm{M}_\odot$ star on the subgiant branch. The grey area is the convective envelope.

Motivations

- Mass transfer stability plays a large role in the production of BH-BH Mergers.
- A common envelope event requires dynamically unstable mass transfer, if the system has stable mass transfer the binary is too wide to merge in Hubble time.

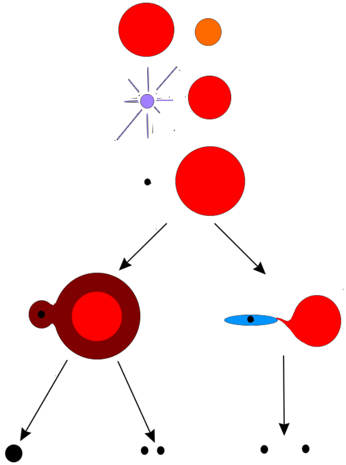

Motivations

- Using the mass transfer prescription described, Belczynski et al. (2016) predicted a BH-BH merger rate of $\gtrsim 1000\ \mathrm{Gpc}^{-3}\mathrm{yr}^{-1}$.
- Predicted merger rate of $12 - 213\ \mathrm{Gpc}^{-3}\mathrm{yr}^{-1}$ by Abbott et al. (2017).

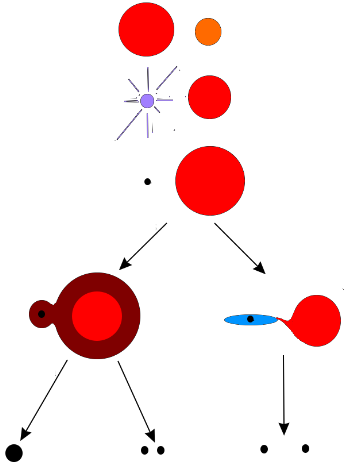

Overview of Improvements

- Use a mass transfer prescription developed by Pavlovskii and Ivanova (2015) with the key features:
  - A more detailed treatment of the outer super-adiabatic layer.
  - Use of detailed geometry in calculating the nozzle size at the L_1 Lagrange point.
- These additions result in new stability criteria:
  - If the L_2 point does not overflow.
  - Or, if the parameters of the binary are not rapidly changing.

Super-adiabatic Response

- The surface layer of the star may react to changes on a time scale shorter than the adiabatic response.
- Stability regions are underestimated in stars with convective envelopes and overestimated in stars with radiative envelopes.

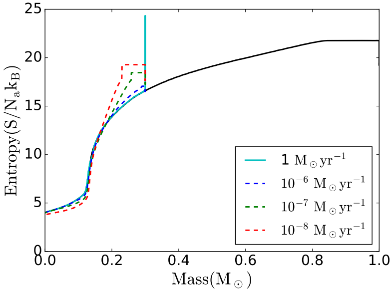

Figure: The entropy profile of a $1\ M_\odot$ star losing mass until reaching $0.3\ M_\odot$ at a variety of mass transfer rates.

Improved Geometry Calculation

- The Roche geometry is calculated with higher order terms resulting in more detailed geometry.
- Higher order terms play a large role in the calculation near the L_1 point.

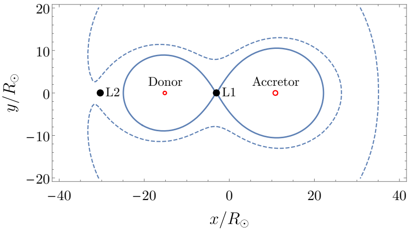

Figure: Roche lobe schematic in the x-y plane with a 1.4 $\mathrm{M}_\odot$ accretor and a 1.0 $\mathrm{M}_\odot$ donor, initial separation of 26 $\mathrm{R}_\odot$.

Mass Transfer From Massive Giants

- Use the improved mass transfer prescription to test the stability of mass transfer from a massive donor.
- These systems are possible progenitors of black hole-black hole mergers.

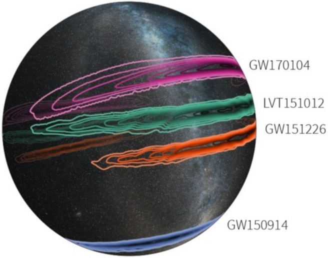

Figure: Map of GW detections.

Stability Region

- During binary evolution, there are two key points of instability that we will denote with radii values (Pavlovskii et al., 2017):
  1. Expansion Instability ($\mathrm{R_S}$): This occurs if mass transfer starts as the donor is experiencing thermal timescale expansion.
  2. Convective Instability ($\mathrm{R_U}$): This occurs if mass transfer starts after the donor has developed a deep convective envelope.
- Stable if mass transfer occurs when $\mathrm{R_S} < \mathrm{R_d} < \mathrm{R_U}$.
- Test this stability by simulating binaries with a black hole and massive donor.

Stable Mass Transfer

- Solar metallicity stars are more stable to both expansion instability and convective instability.
- Both sets of stars show increased stability with lower mass ratio values.
- A simple relation between stability and other properties was not found.
- Table adapted from Pavlovskii et al. (2017)

$M_{d,ZAMS}$	M_{BH}	R_S	R_U
$Z = 0.1Z_\odot$			
20	7	stable	686-721
30	7	44-51	1004-1111
40	7	309-354	1260-1327
60	7	unstable	
60	10	346-364	1705-1790
60	12	140-156	1768-1879
80	7	unstable	
80	10	stable	2217-2241
80	14	134-155	2122-2179
$Z = Z_\odot$			
20	7	stable	729-743
30	7	stable	1144-1174
40	7	stable	1381-1434
60	10	stable	2035-2172
60	12	stable	2009-2057
80	10	stable	stable
80	14	stable	stable

Gravitational Wave Sources

- Prior to the addition of this stability region Belczynski et al. (2016) predicted a merger rate of $\gtrsim 1000\ \mathrm{Gpc}^{-3}\mathrm{yr}^{-1}$.
- Increased stability region greatly decreased predicted rate to $220\ \mathrm{Gpc}^{-3}\mathrm{yr}^{-1}$.
- The predicted rate from Abbott et al. (2017) is $12 - 213\ \mathrm{Gpc}^{-3}\mathrm{yr}^{-1}$.

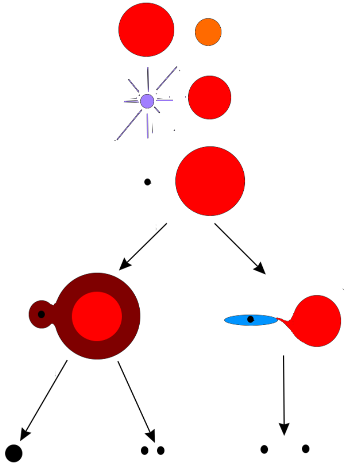

X-ray Luminosity

- Calculating the luminosity of the accretion using:

$$L_X = \epsilon \, \dot{M} c^2$$

- $0.06 \lesssim \epsilon \lesssim 0.42$ for non spinning and maximally spinning black holes.
- With a mass transfer rate of $10^{-7} M_\odot \ yr^{-1}$ produces a luminosity $> 10^{38} erg \ s^{-1}$.

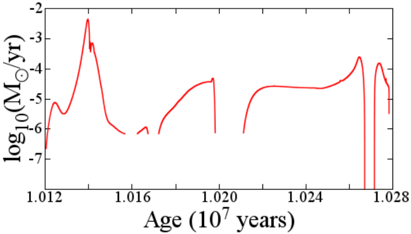

Figure: The mass transfer rate of a $Z = 0.1 \ Z_\odot$ 20 $M_\odot$ giant with a 7 $M_\odot$ black hole.

Ultra Luminous X-ray (ULX) Sources

- Ultra luminous X-ray sources are systems with X-ray luminosities $> 10^{39}\mathrm{erg\ s^{-1}}$.
- Many systems have mass transfer rates consistently exceeding $10^{-6}\mathrm{M_\odot\ yr^{-1}}$ resulting in luminosity $\gtrsim 10^{39}\mathrm{erg\ s^{-1}}$.

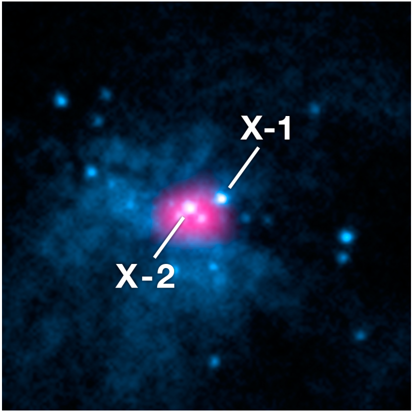

Figure: Image of the ULXs M82 X-1 and X-2

Production Rate

- With the very high mass transfer rates produced by our systems, the luminosity of the binaries peak at $\sim 10^{41}\mathrm{erg\ s}^{-1}$.
- This suggests these binaries may be a formation channel for the most luminous ULXs.
- Expect to produce $\sim$ 0.7 to $\sim$ 1.8 ULXs per star formation unit of $1\ \mathrm{M}_\odot\ \mathrm{yr}^{-1}$.
- Observed systems taken from Gladstone et al. (2013).

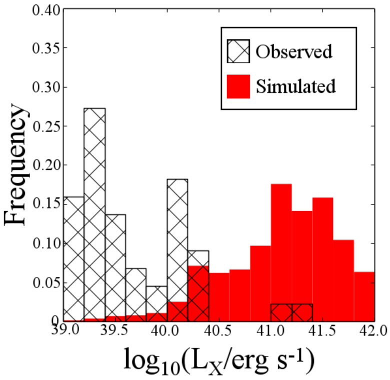

Figure: Normalized histogram of ULX systems.

Summary

- Adiabatic approximation for mass transfer rate underestimates stability in stars with convective envelopes.
- Properly accounting for the readjustment of the surface of the star increases mass transfer stability in systems with high mass transfer rate.
- Applying the improved mass transfer stability to systems originally thought to be progenitors to BH-BH mergers drastically reduces the predicted formation rate.
- The BH-BH progenitors may instead be a formation channel for bright ULX sources.

Thank you

Extra Slides

Multiplicity Fraction

Stellar Class	Mass Range	Percentage	Reference
Very Low Mass	$\lesssim 0.1$	$\sim 22\%$	Allen (2007)
M	$0.01 - 0.5$	$\sim 26\%$	Delfosse et al. (2004)
F - K	$0.7 - 1.4$	$\sim 44\%$	Raghavan et al. (2010)
A	$1.5 - 5.0$	$\gtrsim 50\%$	Duchêne and Kraus (2013)
Early B	$8.0 - 16.0$	$\gtrsim 60\%$	Duchêne and Kraus (2013)
O	$\gtrsim 16.0$	$\gtrsim 80\%$	Chini et al. (2012)

- Percentage given is the fraction of multiple systems in a population. This includes binaries as well as higher order multiples.

Roche Lobe Description

- A 3D representation of the Roche potential of a binary star with q=2 in the corotating frame.

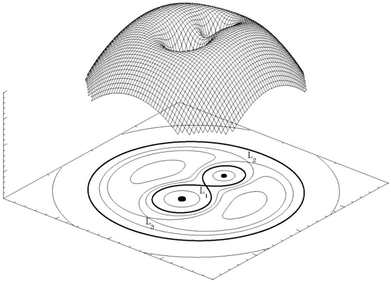

Timescales

- Nuclear Timescale
  $\tau_{\mathrm{nuc}} = \frac{\mathrm{QMc^2}}{\mathrm{L}} \approx 10^{10} \frac{\mathrm{M}}{\mathrm{M_\odot}} \frac{\mathrm{L_\odot}}{\mathrm{L}}\ \mathrm{yr}$
- Thermal Timescale
  $\tau_{\mathrm{therm}} = \frac{\mathrm{E_{th}}}{\mathrm{L}} \approx \frac{\mathrm{GM^2}}{\mathrm{2RL}} \approx 1.5 \times 10^7 \left(\frac{\mathrm{M}}{\mathrm{M_\odot}}\right)^2 \frac{\mathrm{R_\odot}}{\mathrm{R}} \frac{\mathrm{L_\odot}}{\mathrm{L}} \mathrm{yr}$
- Dynamical Timescale
  $\tau_{\mathrm{dynamic}} = \frac{\mathrm{R}}{\mathrm{c_s}} \approx 0.04 \left(\frac{\mathrm{M_\odot}}{\mathrm{M}}\right)^{1/2} \left(\frac{\mathrm{R}}{\mathrm{R_\odot}}\right)^{3/2} \mathrm{day}$

Alternative Formation Channels

- For isolated binaries, the other dominant formation channel is through chemically homogeneous evolution (Mandel and de Mink, 2016).

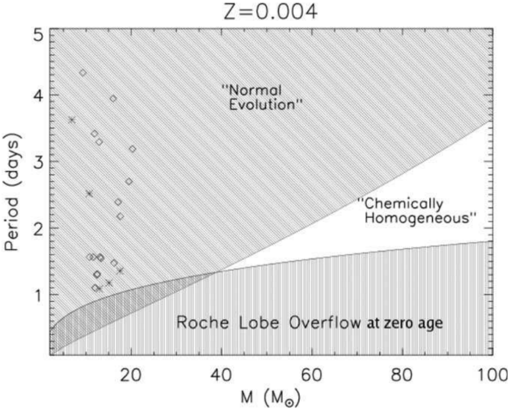

Grazing Encounter Slides

Formation Channel

- The grazing encounter formation channel for a binary system is similar to a tidal capture event.
- The key difference is the tidal capture strips off the entire envelope while the grazing encounter only strips off a portion.
- The resulting binary has a semi-degenerate donor instead of a degenerate donor found in the tidal capture event.

Envelope Stripping

- The envelope stripping requires very high mass transfer rates to produce the desired result.
- In nature the amount of mass lost is effectively instantaneous, stellar evolution codes cannot reproduce this mass loss rate.

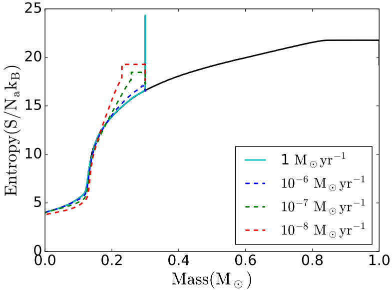

Atmospheric Boundary Conditions

- "Simple Photosphere": No integration, use $\tau = 2/3$ and a constant opacity to calculate.
- "Photosphere Tables": Use a tabulated model for the photosphere.
- "Grey and Kap": Use a model where a grey atmosphere is iterated to find constant pressure, temperature and opacity at surface.
- "Eddington Grey": Integrate hydrostatic balance equations using the Eddington $T - \tau$ relation: $T^4 = \frac{3}{4} T_{\mathrm{eff}}^3 (\tau + 2/3)$.
- $dP_{gas}/d\tau = g/\kappa - (a/3) dT^4/d\tau, \ d\tau = -\kappa \rho dr$

Result: $0.3\ \mathrm{M}_\odot$ Stripped Star

- The stripped stars differ greatly from unperturbed stars of similar color.
- At a color of B-V = 0.8 with $\delta \mathrm{M_V} = \mathrm{M_V^{strip}} - \mathrm{M_V^{norm}}$:
  - $\delta \mathrm{M_V} \gtrsim 2$ for tens of millions of years.
  - $2 \gtrsim \delta \mathrm{M_V} \gtrsim 1$ for $\sim 3 \times 10^8$ years.

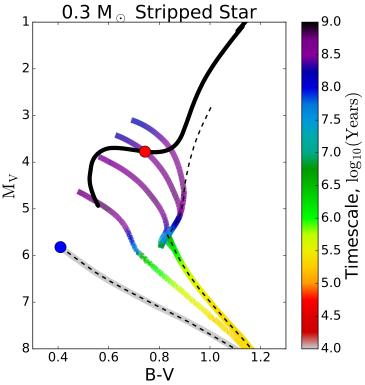

Result: $0.4\ \mathrm{M}_\odot$ Stripped Star

- At a color of B-V = 0.8 with $\delta \mathrm{M_V} = \mathrm{M_V^{strip}} - \mathrm{M_V^{norm}}$:
  - $\delta \mathrm{M_V} \gtrsim 1$ for 1.5×10^8 years.

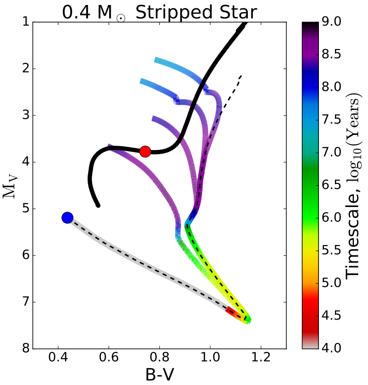

Result: $0.5\ \mathrm{M}_\odot$ Stripped Star

- At redder colors of B-V ~ 1 with $\delta \mathrm{M_V} = \mathrm{M_V^{strip}} - \mathrm{M_V^{norm}}$:
  - $\delta \mathrm{M_V} \gtrsim 2$ for $\sim 8 \times 10^8$ years.

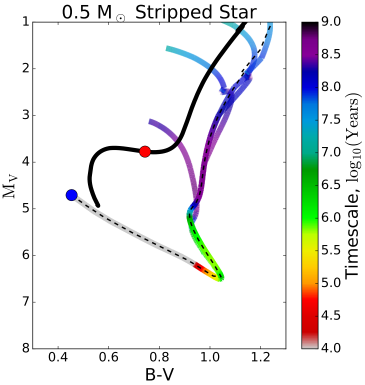

Summary

- Grazing encounters are a possible formation channel for semi-degenerate donor with a compact object.
- This formation channel differs from the standard tidal capture scenario in the amount of donor mass stripped.
  - Tidal capture events strip the entire envelope.
  - Grazing encounters strip a large fraction but not the entire envelope.
- A red underluminous star can be an indicator of the existence of a compact object.

Future Work

Current Research

- Use a 'reverse population synthesis' where we compare current observed low mass X-ray binaries to simulated results.
- Simulations involve an accreting neutron star $1.4\mathrm{M}_{\odot}$ and a donor star ranging from $1-7\mathrm{M}_{\odot}$ at a variety of periods.
- Test these systems with four different magnetic braking schemes and compare the resulting evolutionary tracks.

Magnetic Braking Prescriptions

- Default: $\dot{\mathrm{J}}_{\mathrm{MB,sk}} = -3.8 \times 10^{-30} \mathrm{M_d} \mathrm{R_d^4} \left(\frac{\mathrm{R_d}}{\mathrm{R_\odot}}\right)^{\gamma_{\mathrm{mb}}} \Omega^3 \text{ dyne cm}$
- Wind Boosted: $\dot{\mathrm{J}}_{\mathrm{MB,wind}} = \frac{\dot{\mathrm{M}}_{\mathrm{d}}^{\mathrm{W}}}{\dot{\mathrm{M}}_{\odot}^{\mathrm{W}}} \dot{\mathrm{J}}_{\mathrm{MB,sk}}$
- Convection Boosted: $\dot{\mathrm{J}}_{\mathrm{MB,boost}} = \left(\frac{\tau_{\mathrm{conv}}}{\tau_{\odot\mathrm{conv}}}\right)^{\zeta} \dot{\mathrm{J}}_{\mathrm{MB,wind}}$
- Rotation Saturated: $\dot{\mathrm{J}}_{\mathrm{MB,sat}} = \dot{\mathrm{J}}_{\mathrm{MB,boost}} \times \left(\frac{\Omega}{10\Omega_\odot}\right)^{1.3}$

Test Case: Sco X-1

- Preliminary test case of Sco X-1 was done using the default magnetic braking and a convective boosted magnetic braking.
- Default magnetic braking is not sufficient in reproducing observed values from Sco X-1.

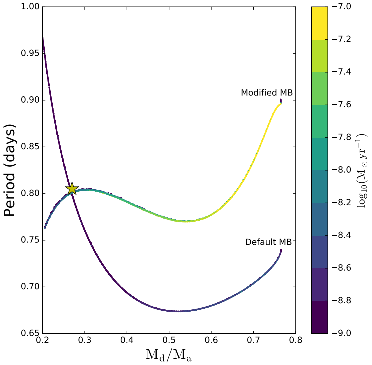

Preliminary Results

- Applying the different magnetic braking schemes to the entire parameter space of interest, we can produce a density plot.
- Assume that the seed period and masses at ZAMS are all equally likely.

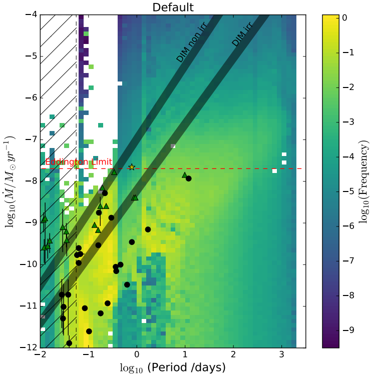

References I

B. P. Abbott, R. Abbott, T. D. Abbott, F. Acernese, K. Ackley, C. Adams, T. Adams, P. Addesso, R. X. Adhikari, V. B. Adya, and et al. GW170104: Observation of a 50-Solar-Mass Binary Black Hole Coalescence at Redshift 0.2. *Physical Review Letters*, 118(22):221101, June 2017. doi: 10.1103/PhysRevLett.118.221101.

H. A. Abt and S. G. Levy. Multiplicity among solar-type stars. *ApJS*, 30:273–306, March 1976. doi: 10.1086/190363.

P. R. Allen. Star Formation via the Little Guy: A Bayesian Study of Ultracool Dwarf Imaging Surveys for Companions. *ApJ*, 668: 492–506, October 2007. doi: 10.1086/521207.

References II

K. Belczynski, S. Repetto, D. E. Holz, R. O'Shaughnessy, T. Bulik, E. Berti, C. Fryer, and M. Dominik. Compact Binary Merger Rates: Comparison with LIGO/Virgo Upper Limits. *ApJ*, 819: 108, March 2016. doi: 10.3847/0004-637X/819/2/108.

R. Chini, V. H. Hoffmeister, A. Nasseri, O. Stahl, and H. Zinnecker. A spectroscopic survey on the multiplicity of high-mass stars. *MNRAS*, 424:1925–1929, August 2012. doi: 10.1111/j.1365-2966.2012.21317.x.

References III

X. Delfosse, J.-L. Beuzit, L. Marchal, X. Bonfils, C. Perrier, D. Ségransan, S. Udry, M. Mayor, and T. Forveille. M dwarfs binaries: Results from accurate radial velocities and high angular resolution observations. In R. W. Hilditch, H. Hensberge, and K. Pavlovski, editors, *Spectroscopically and Spatially Resolving the Components of the Close Binary Stars*, volume 318 of *Astronomical Society of the Pacific Conference Series*, pages 166–174, December 2004.

G. Duchêne and A. Kraus. Stellar Multiplicity. *ARA&A*, 51: 269–310, August 2013. doi: 10.1146/annurev-astro-081710-102602.

P. P. Eggleton. Approximations to the radii of Roche lobes. *ApJ*, 268:368, May 1983. doi: 10.1086/160960.

References IV

J. C. Gladstone, C. Copperwheat, C. O. Heinke, T. P. Roberts, T. F. Cartwright, A. J. Levan, and M. R. Goad. Optical Counterparts of the Nearest Ultraluminous X-Ray Sources. *ApJS*, 206:14, June 2013. doi: 10.1088/0067-0049/206/2/14.

W. Herschel. Catalogue of 500 New Nebulae, Nebulous Stars, Planetary Nebulae, and Clusters of Stars; With Remarks on the Construction of the Heavens. *Philosophical Transactions of the Royal Society of London Series I*, 92:477–528, 1802.

Z. Kopal. The classification of close binary systems. *Annales d'Astrophysique*, 18:379, January 1955.

I. Mandel and S. E. de Mink. Merging binary black holes formed through chemically homogeneous evolution in short-period stellar binaries. *MNRAS*, 458:2634–2647, May 2016. doi: 10.1093/mnras/stw379.

References V

B. D. Mason, D. R. Gies, W. I. Hartkopf, W. G. Bagnuolo, Jr., T. ten Brummelaar, and H. A. McAlister. ICCD speckle observations of binary stars. XIX - an astrometric/spectroscopic survey of O stars. *AJ*, 115:821, February 1998. doi: 10.1086/300234.

K. Pavlovskii and N. Ivanova. Mass transfer from giant donors. *MNRAS*, 449:4415–4427, June 2015. doi: 10.1093/mnras/stv619.

K. Pavlovskii, N. Ivanova, K. Belczynski, and K. X. Van. Stability of mass transfer from massive giants: double black hole binary formation and ultraluminous X-ray sources. *MNRAS*, 465: 2092–2100, February 2017. doi: 10.1093/mnras/stw2786.

References VI

D. Raghavan, H. A. McAlister, T. J. Henry, D. W. Latham, G. W. Marcy, B. D. Mason, D. R. Gies, R. J. White, and T. A. ten Brummelaar. A Survey of Stellar Families: Multiplicity of Solar-type Stars. *ApJS*, 190:1–42, September 2010. doi: 10.1088/0067-0049/190/1/1.

H. Sana, S. E. de Mink, A. de Koter, N. Langer, C. J. Evans, M. Gieles, E. Gosset, R. G. Izzard, J.-B. Le Bouquin, and F. R. N. Schneider. Binary Interaction Dominates the Evolution of Massive Stars. *Science*, 337:444, July 2012. doi: 10.1126/science.1223344.

Figure Credits

Links to images used in presentation in order of appearance. Any images without links are made by myself.

- White Dwarf Binary
- Mass Transferring Binary
- Roche Lobe Example
- Gravitational Wave Map
- Mass Transfer Rate
- Ultra Luminous X-ray Source
- ULX Histogram
- 3D Roche Lobe
- Chemically Homogeneous Evolution